Chemical Bonding

DOI: 10.1002/ange.200705399

Evolution of Chemical Bonding during HCN⇄HNC Isomerization as Revealed through Nuclear Quadrupole Hyperfine Structure**

*Hans A. Bechtel, Adam H. Steeves, Bryan M. Wong, and Robert W. Field**

The making and breaking of bonds in chemical reactions necessarily involve changes in electronic structure. Therefore, measurements of a carefully chosen electronic property can serve as a marker of progress along a reaction coordinate and provide detailed mechanistic information about the reaction. Herein, we demonstrate through high-resolution spectroscopic measurements and high-level ab initio calculations that nuclear quadrupole hyperfine structure (hfs), an indicator of electronic structure, is highly sensitive to the extent of bending excitation in the prototypical HCN⇄HNC isomerization system. Thus, measurements of hfs show how the nature of a chemical bond is altered when a vibration that is coupled to the isomerization reaction coordinate is excited.

Nuclear quadrupole hfs arises from the interaction of a nuclear electric quadrupole moment with the gradient of the electric field at that nucleus. This interaction causes rotational levels to split into multiple components. The magnitude of the splitting is determined by eQq, in which e is the proton charge, Q is the quadrupole moment of the nucleus, and q is the gradient of the electric field ($\partial^2V/\partial z^2$) at the nucleus. The electric quadrupole moment Q is a measure of the departure of the nuclear charge distribution from spherical symmetry and is nonzero for nuclear spins $I \geq 1$. Although Q is constant for a particular nucleus, q can (and generally does) vary in different molecules. These values of q (and hence eQq) report on the local electronic environment of the nucleus, in contrast to Stark effect measurements of the electric dipole moment,[1] which report on the global electron distribution within the molecule.

The HCN⇄HNC isomerization system is a prototypical system for high-barrier, bond-breaking isomerization, a process fundamental to many areas of chemistry, including combustion. The HCN⇄HNC system is also of astrochemical interest because measurements of [HNC]/[HCN] abundance ratios (determined primarily by detecting millimeter-wave emission) provide insights into the chemistry of dark interstellar clouds. Herein, we present the first laboratory measurements of HNC hyperfine structure in vibrationally excited states and extend the measurements of HCN hyperfine structure to higher vibrational levels. These results will allow more precise astronomical measurements of abundance ratios.[2]

In $HC^{14}N$ and $H^{14}NC$, the only nucleus with a nonzero quadrupole moment Q is ^{14}N. The interaction of the nuclear spin ($I_N = 1$) with the rotational angular momentum ($\boldsymbol{J}$) causes the $J = 1$–0 rotational transition for both $HC^{14}N$ and $H^{14}NC$ to split into three lines that are labeled according to the total angular momentum $\boldsymbol{F} = \boldsymbol{I} + \boldsymbol{J}$ and have an intensity ratio of 3:5:1. Figure 1 shows the $J = 1$–0 rotational absorption spectra of several bend-excited levels of $HC^{14}N$ and $H^{14}NC$. These spectra are obtained in a coaxial millimeter-wave pulsed jet spectrometer,[3] which provides better resolution than the conventional orthogonal geometry by minimizing Doppler and transit-time broadening.

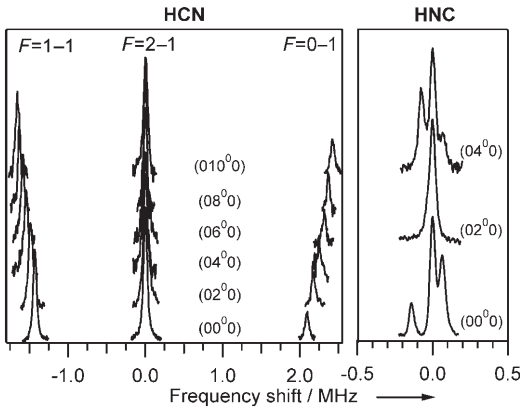

Figure 1. Millimeter-wave rotational spectra ($J = 1$–0) of several bend-excited, $(0\nu_2^{\ell}0)$ vibrational levels of HCN and HNC, where ν_2 is the number of quanta in the bending vibrational mode, and ℓ is the quantum of vibrational angular momentum. Only one of the Doppler-split peaks is shown. The frequencies have been shifted such that the $F = 2$–1 components are aligned at zero frequency shift.

As shown in Figure 1, the hfs patterns of HCN and HNC are qualitatively different. First, the sign of the splitting for the ground vibrational level (00^00) of HNC is reversed with respect to HCN: the weak $F = 0$–1 component for HNC is on the low frequency side of the strong $F = 2$–1 component rather than on the high frequency side as in HCN. Second, the size of the splitting is an order of magnitude smaller for HNC than for HCN. Indeed, the hfs of HNC cannot be resolved

[*] Dr. H. A. Bechtel,[+] A. H. Steeves, Prof. R. W. Field
Department of Chemistry, Massachusetts Institute of Technology
Cambridge, MA 02139 (USA)
Fax: (+1) 617-253-7030
E-mail: rwfield@mit.edu
Homepage: rwf.mit.edu

Dr. B. M. Wong
Materials Chemistry Department, Sandia National Laboratories
Livermore, CA 94551 (USA)

[+] Present address: Advanced Light Source Division
Lawrence Berkeley National Lab, Berkeley, CA 94720 (USA)

[**] This work was supported by the Office of Basic Energy Sciences of the US Department of Energy (DE-FG0287ER13671) and the Donors of the American Chemical Society Petroleum Research Fund.

Supporting information for this article is available on the WWW under http://www.angewandte.org or from the author.

under normal Doppler-broadened conditions.[3] Finally, bending excitation in HCN increases the splitting of the hyperfine components, whereas bend excitation in HNC causes the splitting to decrease initially in magnitude and reverse sign.

To explain these trends, we performed ab initio calculations at the CCSD(T)/cc-pCVQZ level. By choosing a grid of 24 angles between the HCN ($\theta = 0°$) and HNC ($\theta = 180°$) isomers and optimizing all other internal coordinates to minimize the total energy, we obtained a one-dimensional potential from which $(eQq)_N$ values are calculated. Herein, θ is the Jacobi angle between the two Jacobi vectors $\boldsymbol{r}$ and $\boldsymbol{R}$, where $\boldsymbol{r}$ is the N–C displacement vector and $\boldsymbol{R}$ is displacement vector between the C–N center of mass and the H atom. As shown in Figure 2a, the trends in the ab initio $(eQq)_N$ values agree with the experimental observations: $(eQq)_N$ for HCN is large and negative, and $(eQq)_N$ for HNC is small and positive. Bending on the HCN side causes $(eQq)_N$ to increase initially in magnitude, whereas bending on the HNC side causes $(eQq)_N$ to decrease in magnitude and then change sign.

To make quantitative comparisons with the experimental data, the ab initio values of $(eQq)_N$ were averaged over the one-dimensional vibrational wavefunctions. To obtain the experimental $(eQq)_N$ values, the frequencies of the three $J = 1$–0 hyperfine components from each spectrum were fit with the SPFIT program.[4] As shown in Table 1, the agreement between the experimental and ab initio $(eQq)_N$ values is better than 35 kHz, which is remarkable considering the approximation of the motion to a single coordinate.

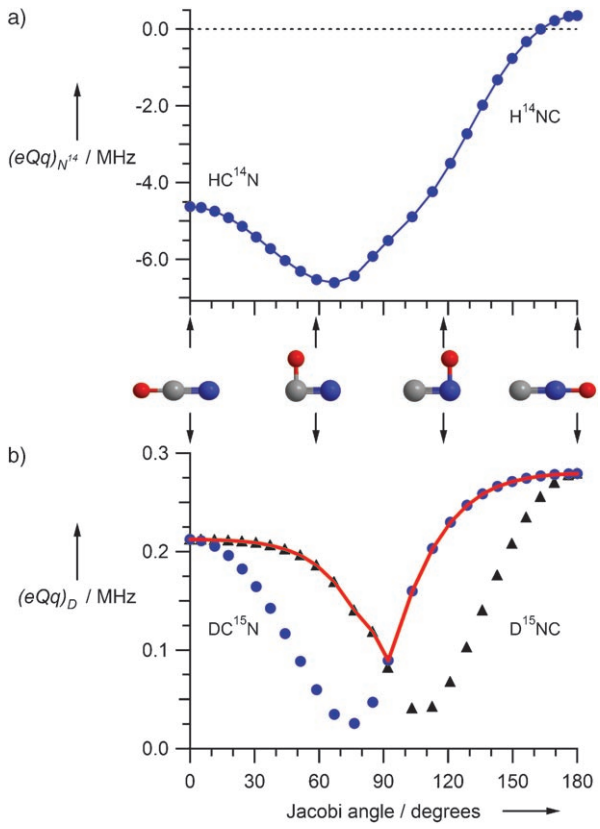

Figure 2. a) Ab initio $(eQq)_N$ values in the C–N bond axis frame as a function of Jacobi angle. b) Ab initio $(eQq)_D$ values in the C–D bond axis frame (black triangles) and the N–D bond axis frame (blue circles). The red line follows the $(eQq)_D$ values in the C–D bond axis frame for $\theta < 90°$ and follows the $(eQq)_D$ values in the N–D bond axis frame for $\theta > 90°$.

Table 1: Experimental and ab initio $(eQq)_N$ values for $H^{14}N^{12}C$ and $H^{12}C^{14}N$.

	Vibrational Level	Experimental [MHz][a]	Ab initio [MHz]
$H^{14}N^{12}C$	(00^00)	0.2641(10)	0.2961
	(02^00)	0.0451(17)[b]	0.0611
	(04^00)	−0.2066(8)	−0.1915
$H^{12}C^{14}N$	(00^00)	−4.7084(11)	−4.6764
	(02^00)	−4.8966(21)	−4.8771
	(04^00)	−5.0699(63)	−5.0561
	(06^00)	−5.2175(68)	−5.2157
	(08^00)	−5.3485(41)	−5.3578
	(010^00)	−5.4579(107)	−5.4843

[a] Values in parentheses represent 95% confidence intervals of replicate measurements in units of the last digit. [b] Value based on line-shape analysis; lack of resolvable hyperfine components and instrumental resolution indicate that $-0.060 < (eQq)_N < 0.060$ MHz.

According to the model of Townes and Dailey,[5] the primary contribution to q in most molecules is the unequal filling of p orbitals in the valence shell of the coupling atom. In H–C≡N:, the bonding associated with the N nucleus consists of an electron in an sp-hybridized orbital that contributes to a σ bond, two electrons in a counter-hybridized sp orbital to make up the lone pair, and one electron in each of the p_x and p_y orbitals for the two π bonds. The lone-pair electrons create an excess of electrons along the C–N axis, resulting in a large negative quadrupole coupling constant. In contrast, the N bonding for the primary resonance structure of $H-\overset{+}{N}\equiv\overset{-}{C}:$ consists of one electron in an sp-hybridized orbital that contributes to the N–C σ bond, one electron in a counter-hybridized sp orbital to make the N–H σ bond, and one electron in each of the p_x and p_y orbitals for the two π bonds. In this case, the four covalent bonds lead to a balance of p electrons and an $(eQq)_N$ near zero. The small positive value arises from the contribution of the secondary resonance structure $H-\ddot{N}=C:$, which has a lone pair in the p_x orbital, causing an excess of electrons perpendicular to the C–N axis.

As Figure 2a demonstrates, the values of $(eQq)_N$ do not follow a simple linear function as the bend angle increases. Instead, bending of HCN initially causes the magnitude of $(eQq)_N$ to increase before eventually decreasing during the isomerization process. Yarmus[6] suggested that effect of bending on $(eQq)_N$ was caused by a decrease in the sp hybridization of the N–C σ bond. A natural bond orbital[7] analysis of our ab initio calculations shows, however, that the hybridization changes associated with the N atom are too small to account for this initial increase. Rather, the increase in magnitude of $(eQq)_N$ is caused by a partial localization of the in-plane π bond on the C atom that removes some of the electron density in the N-atom p_x orbital. Because the lone-pair electrons on the N atom remain primarily along the C–N axis, an even larger p-electron imbalance is created, causing $(eQq)_N$ to increase. In the region around $\theta = 90°$, however, the C–H bond breaks and the N–H bond forms. This rearrangement of the chemical bonding shifts the lone-pair electrons off

the C–N axis and involves them in the four covalent bonds, ultimately leading to a balance of the p electrons and a decrease in $(eQq)_N$.

The nature of the bonding may also be observed from the perspective of the hydrogen nucleus. Although hydrogen does not have a nuclear quadrupole moment ($I_H = {}^1/_2$), deuterium ($I_D = 1$) does. The Townes–Dailey model[5] is not directly applicable for predictions of $(eQq)_D$ because deuterium does not have any p electrons and its one electron is in a spherically symmetric 1s orbital. Instead, the electric field gradient q arises from the nuclear charge and the electron density of the atom to which the deuterium is bound.[8] To simplify the experimental analysis, we examined the $D^{15}NC$ isotopologue instead of the $D^{14}NC$ isotopologue, because ^{15}N ($I = {}^1/_2$) does not have a nuclear quadrupole moment; thus, the hfs of $D^{15}NC$ gives a direct measure of $(eQq)_D$. The experimental and ab initio values for the ground vibrational state of $D^{15}NC$ are 255.0(38) and 270.4 kHz, respectively. The $J = 1$–0 transition of $DC^{15}N$ is just outside the range of our spectrometer, but the literature value[9] of $(eQq)_D = 200.9(8)$ kHz is in good agreement with our ab initio calculation of $(eQq)_D = 208.9$ kHz. Unlike $(eQq)_N$, $(eQq)_D$ is similar in sign and magnitude for the two isomers. Moreover, as shown in Figure 2b, the ab initio values of $(eQq)_D$ remain relatively unchanged as the molecule bends, except for the region around $\theta = 90°$, where the C–D and N–D bonds are not well defined. The lack of change in $(eQq)_D$ indicates that the chemical bond involving deuterium remains relatively unaltered until isomerization begins when the D nucleus bridges the C and N nuclei. Because q originates primarily from the interaction with the nucleus to which deuterium is bound, we expect q to be largely dependent on the bond length.[10] Indeed, the ab initio $(eQq)_D$ values are strongly anticorrelated with bond length: the smallest $(eQq)_D$ value occurs at $\theta = 90°$, which corresponds to the largest separation between D and C or N.

We have demonstrated that nuclear quadrupole hfs is altered by the extent of bending excitation in HCN and HNC. As shown in Figure 3, the ab initio $(eQq)_N$ values of $HC^{14}N$ and $H^{14}NC$ follow the patterns experimentally established at low excitation and change smoothly as a function of increasing energy in the bending coordinate. Near the isomerization barrier (above 15000 cm^{-1}), however, the $(eQq)_N$ values of $HC^{14}N$ and $H^{14}NC$ deviate dramatically from their respective trends before approaching a nearly constant value at above barrier energies. The deviation is caused by the onset of delocalization of the vibrational wavefunction into the regions above both the HCN and HNC potential energy wells. Bowman et al.[1] proposed the use of the electric dipole moment, another electronic structure indicator, as a diagnostic for delocalized states, because the HCN and HNC isomers have large dipole moments of nearly equal magnitude, but opposite sign, and the delocalized states have dipole moments near zero. Stark effect measurements of the dipole moment can consequently characterize the degree of localization in a vibrational state of HCN or HNC. Although a single measurement of nuclear quadrupole hfs is not as useful as a single Stark effect measurement in terms of identifying a delocalized level, hfs can determine whether the wavefunction is localized in the HCN or HNC potential well, which is not possible with a single Stark effect measurement. Moreover, the dramatic deviation from the $(eQq)_N$ trend along a progression of bending vibrational levels provides a useful indicator of the onset of delocalization and provides a means of identifying pre-delocalized levels. Thus, Stark effect and nuclear quadrupole hfs measurements are complementary indicators of electronic structure that can be used as diagnostics for detecting and assigning delocalized states. Because the lowest energy delocalized state is the isomerization transition state, the detection of this state is tantamount to catching the molecule in the act of bond-breaking isomerization.

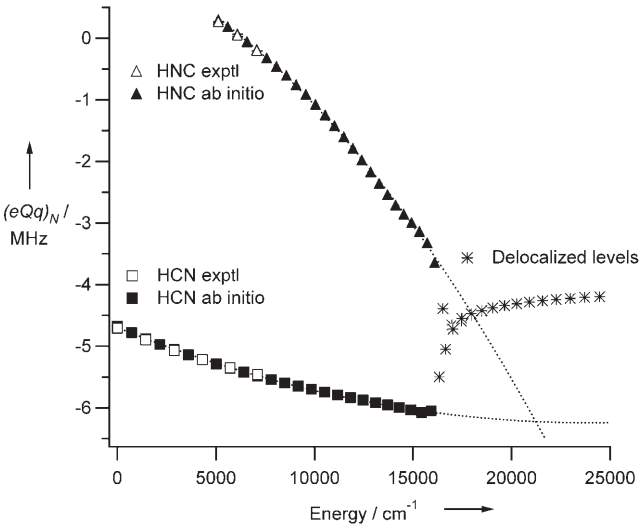

Figure 3. Experimental and vibrationally averaged ab initio $(eQq)_N$ values for $HC^{14}N$ and $H^{14}NC$ in the principal inertial axis frame, which is approximately aligned with the C–N bond. The ab initio energies are referenced to the HCN(00^00) level, and the experimental $(eQq)_N$ values are matched to the ab initio energies according to vibrational level. The $(eQq)_N$ values for $HC^{14}N$ and $H^{14}NC$ vary smoothly as a function of energy until the onset of delocalization, at which point they deviate dramatically.

Experimental Section

The absorption measurements are performed in a coaxial mm-wave jet spectrometer, which has been described previously.[3] Vibrationally excited HCN and HNC are generated either through an electric discharge of a 2% acetonitrile/Ar mixture or through 193-nm photolysis of a 2% acrylonitrile/Ar mixture. The pulsed nozzle is attached to an aluminum rooftop reflector, which has a small hole for the molecular beam. The mm-wave radiation is produced by a W-band (72–106 GHz) Gunn oscillator that is phase-locked to the tenth harmonic of a microwave synthesizer (HP 8673E). The radiation is emitted into free space through a standard gain pyramidal horn and propagated through a wire-grid polarizer oriented to pass the linearly polarized mm-wave radiation. A polytetrafluoroethylene (PTFE) lens ($f = 30$ cm) is used to roughly collimate the mm-wave radiation, which is counterpropagated with the molecular beam and directed onto the rooftop reflector oriented at 45° with respect to the polarization of the mm-wave radiation. The rooftop reflector rotates the mm-wave polarization by 90° and reflects the mm-wave radiation back onto itself, making a second pass of the vacuum chamber. The mm-wave radiation is focused by the PTFE lens, and finally reflected

by the polarizer onto a liquid-helium-cooled InSb hot electron bolometer (Cochise Instruments). The coaxial geometry of the mm-wave radiation and the molecular beam results in two Doppler-split peaks, the frequencies of which are averaged to determine the rest frequency.

Received: November 24, 2007
Published online: March 10, 2008

Keywords: ab initio calculations · gas-phase reactions · isomerization · reaction mechanisms · rotational spectroscopy

[1] J. M. Bowman, S. Irle, K. Morokuma, A. Wodtke, *J. Chem. Phys.* **2001**, *114*, 7923.
[2] B. E. Turner, *Astrophys. J. Suppl. Ser.* **2001**, *136*, 579.
[3] H. A. Bechtel, A. H. Steeves, R. W. Field, *Astrophys. J.* **2006**, *649*, L53.
[4] H. M. Pickett, *J. Mol. Spectrosc.* **1991**, *148*, 371.
[5] C. H. Townes, B. P. Dailey, *J. Chem. Phys.* **1949**, *17*, 782.
[6] L. Yarmus, *Phys. Rev.* **1956**, *104*, 365.
[7] E. D. Glendening, K. B. J, A. E. Reed, J. E. Carpenter, J. A. Bohmann, C. M. Morales, F. Weinhold, Theoretical Chemistry Institute, University of Wisconsin, Madison, **2001**.
[8] M. Rinne, J. Depireux in *Advances in Nuclear Quadrupole Coupling*, *Vol. 1* (Ed.: J. A. S. Smith), Heyden, New York, **1974**, pp. 357.
[9] G. Cazzoli, C. Puzzarini, J. Gauss, *Astrophys. J. Suppl. Ser.* **2005**, *159*, 181.
[10] H. Huber, *J. Chem. Phys.* **1985**, *83*, 4591.

